Indian Journal of Radio & Space Physics
Vol. 3, September 1974, pp. 273-277

Solar Activity Variation of Electron & Ion Temperatures in Equatorial Topside Ionosphere

RISAL SINGH & B. C. NARASINGA RAO

Radio Science Division, National Physical Laboratory, New Delhi 110012

Received 18 *September* 1973

The daytime electron and ion temperature (T_e and T_i) profiles in the topside ionosphere in the equatorial region are theoretically investigated for low and medium solar activity conditions. The available ion composition data from incoherent back-scatter radar and satellite *in situ* measurements are used in studying the thermal structure. The local and non-local electron heating rates due to photoelectrons are evaluated for these solar activity conditions. The results show that the plasma temperature at 400 km as well as at 1000 km increases from low to medium solar activity conditions, while it decreases at 700 km. The altitudinal extent of isothermal region around 500 km increases with increasing solar activity and the temperature gradient above the isothermal region is lower for medium solar activity as compared to low solar activity. The calculated temperature profiles are in fair agreement with the direct measurements of T_e and T_i taken at Jicamarca for similar conditions.

1. Introduction

THE DIRECT measurements on the daytime electron and ion temperature (T_e and T_i) distributions in the topside equatorial ionosphere for low and medium solar activities are available at Jicamarca[1-3] for August 1965 and May 1967; the monthly average values of solar flux $S_{10.7}$ for these two months were 70 and 140 units respectively. Measurements of T_e at 1000 km are also available from satellite measurements for low and medium solar activity (Brace *et al.*[4]). The main differences in the features of the electron temperature profiles, concluded from above experimental results, for low and medium solar activities in the topside equatorial ionosphere are:

(i) At 400 km, T_e is greater at medium solar activity being about 1350°K compared to 1000°K for low solar activity. On the other hand, at 700 km, T_e is lower for medium activity (1200°K) compared to that for low activity (1800°K). Again, at 1000 km, T_e is greater for medium activity than for low activity (2200°K and 1800°K respectively).

(ii) The isothermal region, where $T_e = T_i = T_n$ (T_n is the neutral temperature), becomes wider and its both lower as well as upper boundaries shift to higher altitudes as the solar activity increases. The isothermal region extends from 300 to 500 km for low activity while it extends from 450 to 700 km for moderate activity.

(iii) The temperature gradient above the isothermal region is *more* for *low* solar activity than for medium activity. The purpose of the present study is to estimate theoretically the temperature profiles in the topside equatorial ionosphere for low and moderate solar activities with a view to find out whether these experimental results can be accounted for by the current theory. The theoretical calculations are described in detail and the results are compared with the observations taken during similar conditions.

2. Method of Investigation

The method of investigation is similar to that adopted by the authors in their earlier work (Rao and Singh[5]). In the topside ionosphere the steady state electron temperature distribution is determined by the heat conduction equation which is given by :

$$-\frac{d}{ds}\left(K_e \frac{dT_e}{ds}\right) = Q - L_e \qquad ...(1)$$

where K_e is the thermal conductivity of electrons given by $7{\cdot}7 \times 10^5 \times T_e^{5/2}$ eV cm^{-1} sec^{-1}deg^{-1}, Q is the heat input rate to electrons, L_e is the rate of heat loss from electrons and S is the distance along the geomagnetic field line.

In the topside ionosphere above 400 km the collisional heat loss rate from electron to ions (L_{ei}) predominates over that from electrons to neutrals (L_{en}). So in this region almost all the heat energy from electrons is transferred to ions which in turn loose this energy to the neutrals through the collisional processes. Since the thermal conduction of ions is relatively small, the ion temperature may be obtained by the equation :

$$L_{ei} = L_{in} \qquad ...(2)$$

where L_{in} is the collisional heat loss rate from ions to neutrals. The functional forms and the coefficients in the collisional loss rates are taken from Banks[6]. Since the geomagnetic field lines are more curved in

the equatorial region, Eq. (1) is solved along the different magnetic field lines to get the vertical temperature profiles over the equator. Details of the calculations of temperature profile for low solar activity are given in our previous work[5]. Similar procedure is adopted here for medium activity calculations.

3. Estimation of Q and L

To study the variation of thermal structure with solar activity one should find out the variation of various parameters, i.e. the electron heat input rate Q, the electron collisional heat loss rate L_e and the ion collisional heat loss rate L_{in}, occurring in Eqs. (1) and (2). The heat input rate Q consists of Q (local) due to locally produced photoelectrons and Q (non-local) due to photoelectrons coming from lower regions. The local heating rate Q (local) is equal to the product of photoelectron production rate and the heating efficiency (the energy input to the ionospheric electron gas per electron-ion pair formed). It decreases with altitude in the topside ionosphere due to the decrease in photoionization rates since the heating efficiency is almost constant at these altitudes. Since the photoionization rates decrease due to the decrease in the density of ionizable neutral constituent n (O), it is safe to assume that the local heating rates decrease with the decrease in the density of the atomic oxygen in the topside ionosphere. When the intensity of ionizing solar radiations and the density of the atomic oxygen increase with solar activity, the net effect is the increase in the photoionization rates and hence increase in Q (local). Since the photoelectron fluxes and the electron density increase with the increasing solar activity[7], the non-local heating rates will also increase for higher activity.

Swartz[8] has made detailed calculations on daytime heat input rates to ambient electrons for medium solar activity (monthly average solar flux $S_{10.7} = 150$ units in the F-region up to 370 km. These rates include both the Q (local) and Q (non-local) but at heights below 300 km, particularly in equatorial region where local conditions for heating rates are maintained to relatively greater heights, the Q (non-local) is negligible. So the total heating rates are taken as equal to Q (local) at 300 km and these values are extrapolated to higher altitudes with proper atomic oxygen scale height. The non-local heat input rates at and above 400 km are calculated from the measured photoelectron fluxes[9,10], and the electron density profiles are taken by Alouette-II[11] and Jicamarca radar observatory[12].

The various heating rates are shown in Fig. 1 along with those for low solar activity adopted from Nagy

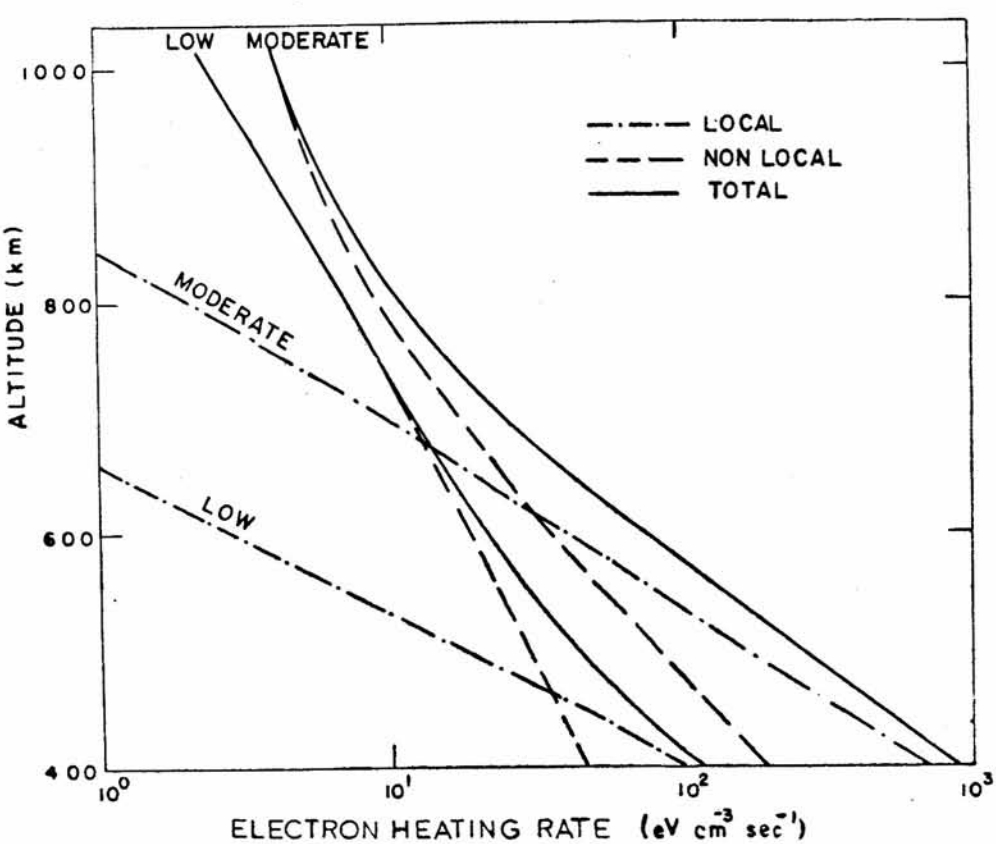

Fig. 1—Altitude variation of electron heating rates, Q_e, for low and medium solar activities (The local and non-local heating rates are also shown separately)

et al.[13]. It is evident from Fig.1 that the heating rates are one order higher for medium activity than for low activity at 400 km while at 1000 km the heating rates are higher only by a factor of 2 or so. Secondly, the level where the local and non-local heating rates become equal, shifts to the higher altitude as the solar activity increases. So the criterion that the local heating rates can be taken as the total heating rates, is valid up to higher altitudes for medium solar activity compared to lower activity.

The electron collisional loss rate (L_e) in the topside ionosphere depends on the electron and relative ion densities because the collision cross-section is different for different ions. The main ions in the region of interest here are O^+, H^+ and He^+. The He^+ remains only as a minor ionic constituent and so the relative densities of O^+ and H^+ are the main controlling factors of loss rates. The ion density profiles along the geomagnetic field lines are required in our study, but these are not readily available from any measurements. Therefore, to construct these profiles we have combined the altitudinal and latitudinal distribution of electron and ion density measurements from incoherent backscatter and satellite measurements. For low solar activity the average electron density contours observed with Alouette-I in equatorial region (Chan and Colin[14]) are used to obtain the electron density profiles along various magnetic field lines and the percentages of O^+, $H^+$and He^+ are obtained for various geomagnetic latitudes in the topside equatorial ionosphere by interpolating the observed percentages of these ions at Jicamarca[1] and Arecibo[15]. For medium solar activity the electron density data taken by Alouette-II[11] and Jicamarca radar observatory[12] and ion density data from OGO 4 results (Taylor[16]) are used to construct the electron and ion density profiles along various magnetic field lines. Taylor's results for ion densities are available only at one altitude in the range of 400-1000 km for a particular geomagnetic latitude. So the ion densities at other altitudes below and above this altitude for the same geomagnetic latitude have to be extrapolated taking into account the nature of variation. This is done due to the non-availability of any other altitudinal profiles of data for medium solar activity. These extrapolations evidently put a limit on the accuracy of the calculated temperature profiles.

The above mentioned ion density profiles are constructed along the magnetic field lines increasing in L value from 1·08 to 1·16. These field lines reach altitudes of 510 to 1020 km over the equator and provide the necessary data to get the temperature profile upto 1000 km over the equator. For example, the profiles along $L = 1{\cdot}16$ for low and moderate solar activity are shown in Fig.2. It may be noted that transition level from O^+ to H^+ increases in altitude as the solar activity increases. This is because of the decrease in the netural hydrogen density with increasing neutral temperature for increasing solar activity. About He^+ no definite conclusion should be drawn here because they are constructed from approximate data for low activity. These uncertain values of He^+ density will, however, not affect the final calculations of tempera_

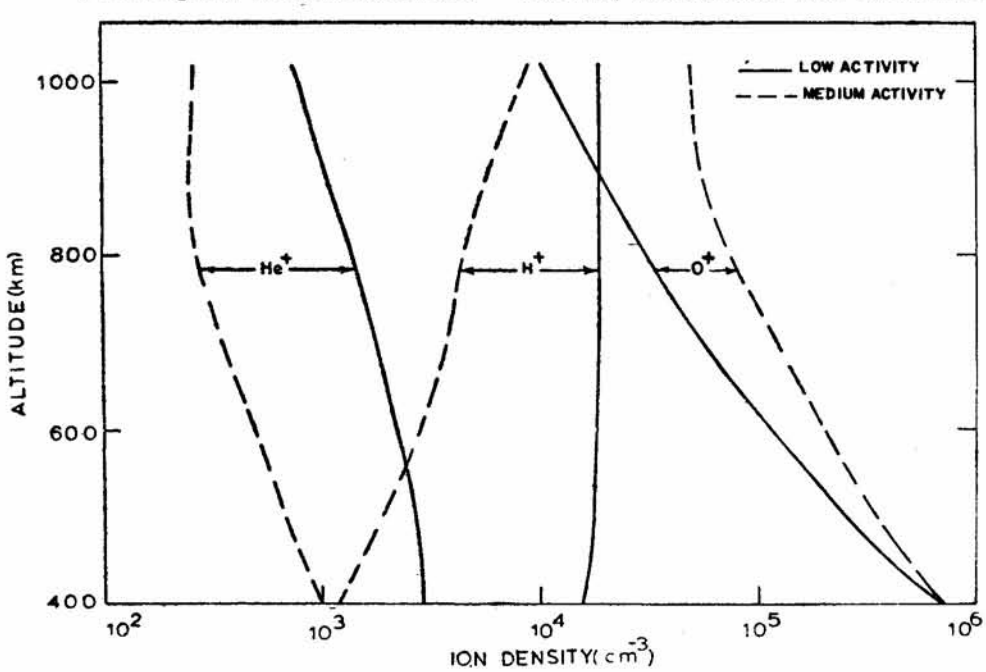

Fig. 2—The computed ion density profiles along the geomagnetic field line $L = 1.16$ for low and medium solar activities (These profiles are obtained by combining the available data of Alouette-II, OGO4 and incoherent backscatter data over Jicamarca.)

tures because the concentration of these ions is very small in comparison to other two major ions.

4. Results and Discussion

Knowing the heating rates and ion composition profiles required for loss rates (and their variation with solar activity) along the various magnetic field lines, the heat conduction equation for electrons and heat balance equation for ions are solved to get the electron and ion temperatures. The neutral composition from Jacchia[17] model atmosphere corresponding to exospheric temperatures 900 and 1100°K are taken for low and medium solar activity conditions respectively. These temperatures roughly correspond to periods of plasma temperature profiles at Jicamarca[3] for low and medium solar activities used for comparison of the theoretically calculated results with the observed ones. The boundary conditions to get the exact solutions are: (i) the heat flux flowing down the field line at the equator is zero, and (ii) T_e is determined at the lower boundary of the field line at 400 km by local heat balance between Q and L_e.

The calculated temperature profiles along the field line $L = 1{\cdot}16$ for low and medium solar activities are shown in Fig.3. The different profiles show that: (i) temperatures are higher for medium solar activity, T_e being 950 and 1350°K at 400 km; and 1000 and 2150°K at 1000 km for low and medium solar activities respectively; (ii) T_e is more closely coupled to T_i at 400 km for low solar activity than for medium activity, the difference $(T_e - T_i)$ being about 20°K for low activity and about 170°K for medium activity. However, they are almost equally coupled to each other at 1000 km where the difference is less than 50°K; and (iii) T_i is closer to T_n for low solar activity at 400 km than that for moderate activity. The difference $(T_i - T_n)$ is only 20°K for low activity while it is 60°K for moderate activity.

From the calculated values of T_e and T_i at the

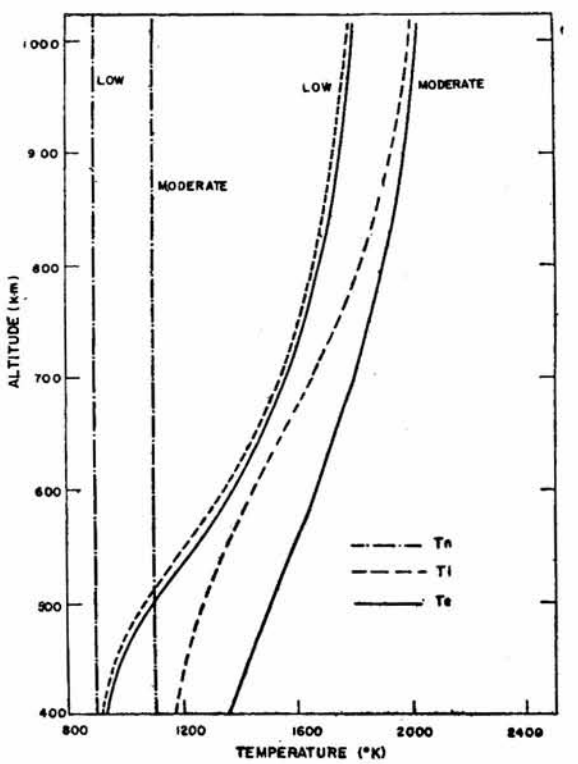

Fig. 3—Calculated electron and ion temperature (T_e, T_i) profiles along the magnetic field line $L = 1.16$ for low and medium solar activities (Note that this field line starts over 17° geomagnetic latitude at 400 km height and reaches 1020 km over the equator. The exospheric neutral temperature, T_n, is also shown for both the activity conditions)

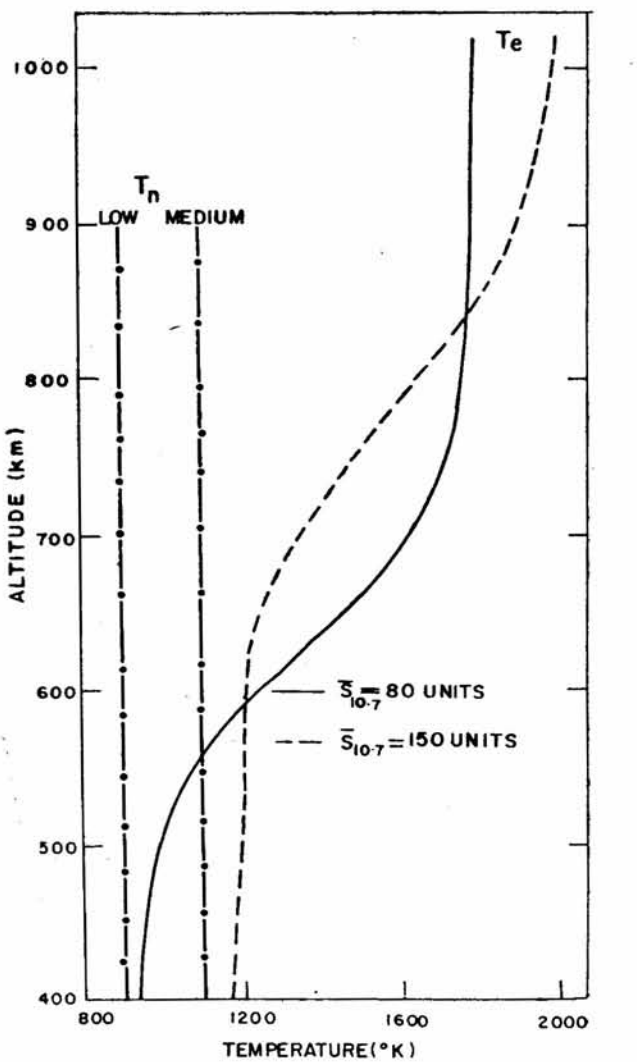

Fig. 4—Theoretically calculated vertical profiles of electron temperature at equator in the topside ionosphere for low and medium solar activities (For the sake of clarity, T_i is not shown here because it is closely coupled to T_e. The exospheric neutral temperature, T_n is also shown for both the solar activity conditions)

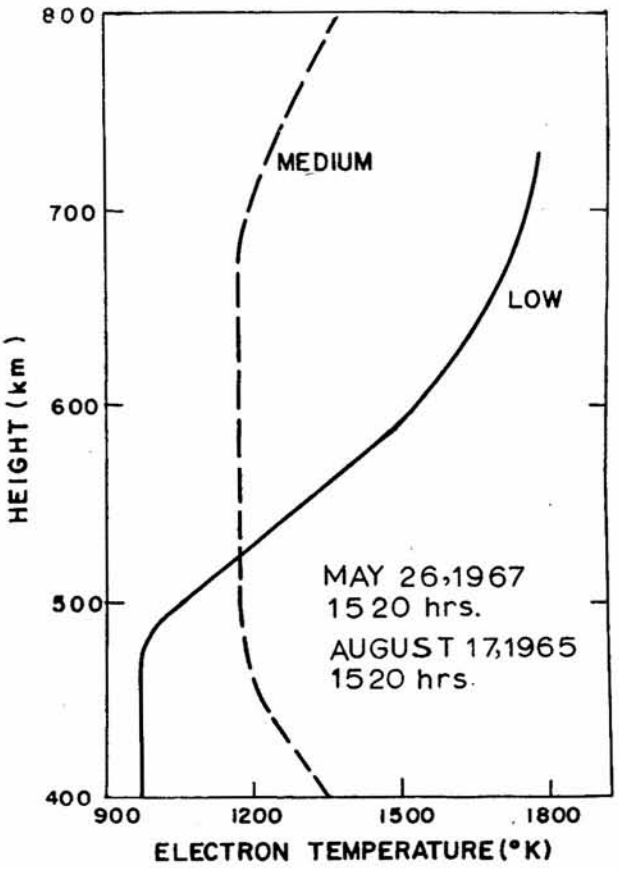

Fig. 5—Observed daytime altitude profiles of electron temperature at Jicamarca in the topside ionosphere for low and medium solar activities (Note that these profiles are similar to those theoretically calculated profiles over the equator and shown in Fig.4.)

apex of different field lines the vertical profiles of T_e and T_i over the equator are constructed. In Fig.4, only the T_e profiles are shown for low and medium solar activities. The ion temperature which closely follows the electron temperature is not shown here. It can be inferred from this figure that the electron temperature is more for medium solar activity at 400 and 1000 km, while at 700 km it is *more* for *low* solar activity than for the medium solar activity. The isothermal region extends up to 500 km for low solar activity while it goes up to 640 km for the medium solar activity. It is also evident from Fig. 4 that the electron temperature gradient above isothermal region is less for medium solar activity than for low activity. For comparison the observed daytime electron temperature profiles[3] for similar conditions are shown in Fig. 5. The theoretical profiles show almost all the features of the experimentally observed profiles. It is concluded that the theoretical temperature model is consistent with the observations.

The results presented above are only for two periods of solar activity. Similar calculations are needed for other periods, specially for high solar fluxes, to cover the whole solar cycle variation of thermal structure. The ion composition profiles used in the above calculations are constructed by doing a number of interpolations and extrapolations, and these may differ from the actual values. Here in this study we have not taken into consideration the latitudinal variation of electron heating rates at fixed altitudes which may be of significant magnitude due to the greater escape probability at medium geomagnetic latitudes than at the equatorial latitudes. A more detailed study is under progress for the variation of thermal structure in the topside equatorial ionosphere as a function of solar activity as more ion composition data is becoming available from observations for high activity periods.

References

1. FARLEY, D. T., MCCLURE, J. P., STERLING, D. L., GREEN, J. L., *J. geophys. Res.*, **72** (1967), 5837.
2. MCCLURE, J. P., *J. geophys. Res.*, **74** (1969), 279.
3. MCCLURE, J. P., *J. geophys. Res.*, **76** (1971), 3106.
4. BRACE, L.H., MAYR, H.G. & REDDY, B.M., *J. geophys. Res.*, **73** (1968), 1607.
5. RAO, B.C.N. & SINGH, R., *Indian J. Radio Space Phys.*, **1** (1972), 151.
6. BANKS, P.M., *J. geophys. Res.*, **72** (1967), 3365.
7. NISBET, J.S., *J. atmos. terr. Phys.*, **30** (1968), 1257.
8. SWARTZ, W.E., *PSU-IRL-SCI 381, Scient. Rep. 381* (Ionospheric Research Laboratory, the Pennsylvania State University, University Park, Pennsylvania 16802), 1972.
9. KNUDSON, W.C., *J. geophys. Res.*, **77** (1972), 1233.
10. CICERONE, R.J. & BOWHIL, S.A., *Radio Sci.*, **6** (1971), 957.
11. *Alouette-II Data, Data on topside ionosphere, electron densities and scale heights from Alouette-II observations over Japan, Vol. 2,* Prepared by Radio Research Laboratories, Tokyo, Japan, 1971.
12. MCCLURE, J.P. & PETERSON, V.L., *Radio Sci.*, **7** (1972), 539.
13. NAGY, A.F., FONTHEIM, E.G., STOLARSKI, R.S. & BEUTLER, A.E., *J. geophys. Res.*, **74** (1969), 4667.
14. CHAN, K.L. & COLIN, L., *Proc. IEEE*, **57** (1969), 990.
15. CARLSON, H.C. & GORDON, W.E., *J. geophys. Res.*, **71** (1966), 5573.
16. TAYLOR (Jr), H.A., *Planet. Space Sci.*, **19** (1971), 77.
17. JACCHIA, L.G., *Smithsonian astrophysical observatory special report 332*, 1971.